Indian Journal of Biochemistry & Biophysics
Vol. 59, April 2022, pp. 455-460

Nano-therapeutic efficacy of green synthesized gold nanoparticles (gAuNPs) and its antibacterial efficacy

Vivan Yagnik Setia[1,2#], Kapil Dangi[1#], Largee Biswas[1], Priyanka Singh[1] & Anita Kamra Verma[1]*

[1]Nano-Biotech Lab, Kirori Mal College, University of Delhi, Delhi-110 007, India

[2]Boston University College of Arts and Sciences, Boston, USA

Received 22 December 2021; *revised 20 February 2022*

We report the efficacy of the gold nanoparticles (AuNPs) synthesized using the leaf extracts of *Syzygium cumini* (common name Jamun) with auric chloride (AuCl4) which was used as both reducing and capping agent at room temperatures- 25°C. Synthesized AuNPs were characterized using UV-Vis spectroscopy indicating a peak in the range of 520-540 nM. The hydrodynamic radii measured by DLS clearly indicated the size of AuNPs in the range of 14-64 nM. The biological efficacy in terms of antimicrobial activity was assessed by the Kirby Bauer method, applied for both Gram-positive and Gram-negative bacteria such as *Staphylococcus aureus* and *Escherichia coli*, respectively. The Zone of inhibition (ZOI) diameter was found to be 4 mM and 3 mM in *S. aureus* and *E. coli*, as indicated by the bactericidal activity. Hence, AuNPs synthesized by green synthesis are proposed as economical, environment friendly with immense potential as an antibacterial agent and for drug delivery.

Keywords: Antibacterial activity, gAuNPs, Surface plasmon resonance

Nanoparticles tend to acquire unique characteristics owing to their increased surface area to volume ratio translating into enhanced anti-microbial and optical properties, coupled with structural strength enhancement properties[1]. Nanoparticles may be broadly divided into an organic group that includes carbon nanoparticles (fullerenes), and an inorganic group that comprises of noble metal nanoparticles (silver and gold), magnetic nanoparticles, and semi-conductor nanoparticles - zinc oxide and titanium oxide. Inorganic nanoparticles of noble metals are gaining popularity as they provide superior physical properties coupled with functional versatility[2]. Among the metal nanoparticles, gold nanoparticles (AuNPs) have generated sufficient interest due to their chemical stability, enhanced conductivity, catalytic and most important antibacterial, anti-fungal, anti-viral, anti-cancer anti-inflammatory activities which can be integrated into composite fibers, cosmetic products, cryogenic superconductors, food industry and electronic components[3-4]. AuNPs have been used for defence against a variety of micro-organisms, and further to combat drug resistance in microbes. AuNPs have remarkable properties that can be exploited for wastewater treatment, agriculture, drug delivery, and biomedical applications.

Metal nanoparticles can be synthesized by both chemical and physical methods including electrochemical reduction[5], chemical reduction[6], heat evaporation[7], and photochemical reduction[8]. Other protocols like gamma radiation, laser ablation, microemulsion, autoclave, and microwaving are efficient methods too but are limited by high operational costs, energy consumption, and use of toxic chemicals[9]. In such a scenario, green synthesis has tremendous potential, as it is cost-effective, environment friendly coupled with an ease of scaling up. Green synthesis would greatly rely on selection of the plant to be used as the reducing agents like citric acid, flavonoids, ascorbic acids, dehydrogenases, reductases and extracellular electron shuttlers that play an essential role for biosynthesis of metal nanoparticles. Plant extracts act as a reducing and capping agent forming stable and shape-controlled AuNPs[10]. The plant-borne biomolecules include reducing agents like enzymes, amino acids, proteins, polysaccharides, vitamins, and organic acids such as citrates that are environmentally benign, yet chemically very complex[11]. In the present work, we propose to synthesize AuNPs from leaves by the use

#Equal first author
*Correspondence:
Phone: +91-9818921222 (Mob)
E-mail: akverma@kmc.du.ac.in

of chemicals, as the leaves themselves contain betulinic acid, β-sitosterol, mycaminose, crategolic (maslinic) acid, n-hepatcosane, n-hentriacontane, n-nonacosane, n-dotricontanol, n-octacosa-nol, n-triacontanol, myricitrin, quercetin, myricetin, and the flavonol glycosides myricetin 3-O-(4"-acetyl)-α L-rhamno-pyranosides that may act as a reducing agent during the synthesis of AuNPs[12]. Temperature-dependent synthesis and characterization of AuNPs from leaf extract of *S. cumini* in terms of its biological efficacy against *S. aureus* and *E. coli* were evaluated[13-14.]

Experimental

Materials

Fresh leaves were obtained from the *S. cumini* tree located in the Institution itself. Nutrient agar, Nutrient broth, Gentamycin, Luria-Bertani Broth were purchased from Hi-Media Laboratories Pvt Ltd (Mumbai,India). Auric chloride ($Aucl_4$), Ethidium bromide (EtBr), Agarose were purchased from Sigma-Aldrich (USA). All the chemicals were used without further purification.

Synthesis of AuNPs

Leaves were scrupulously washed with distilled water and left for air drying. Briefly, 3 g of dried leaves were weighed separately and dissolved in 30 mL of distilled water, and kept at 80°C for 1 h. The extracts thus prepared were cooled and filtered through Whatman's Filter paper no. 1 and stored at 4°C. To 45 mL of 1 mM $AuCl_4$, 5 mL of the above-prepared extract from leaves were added dropwise under vigorous stirring and maintained at room temperature Change in colour was observed slowly from pale yellow to ruby red, which indicated the formation of AuNPs[15].

Characterization of AuNPs

UV visible spectral analysis

Although color change is an indicator of nanoparticle formation, it cannot be the sole reliable parameter indicating the formation of AuNPs, hence the shift in the absorption spectra for AuNPs as observed by UV-Spectrophotometer (Cary-60, Agilent Technologies, USA). The shift in the absorbance spectra indicated the formation of nanoparticles and was compared to spectra of distilled water taken as blank.

Dynamic light scattering

The hydrodynamic radii were analyzed by Dynamic light scattering (DLS) using Zeta-sizer (Nano-ZS, Malvern USA). For the size-based assessment of nanoparticles, the sample solution was diluted (1:9) with deionized water.

Transmission Electron Microscopy

Transmission Electron Microscopy (TEM) was done to examine the size and morphology of the AuNPs. A drop of the aqueous solution containing the AuNPs was placed on the carbon-coated copper grid and dried under an Infra-red lamp. The carbon-coated grids were observed under Technai G2 T-30U-TWIN of FEI.

FTIR analysis

FTIR was used to identify and analyze the functional group and composition of the lyophilized AuNPs responsible for the reduction of Au ion and capping of the bio-reduced gold nanoparticles using Cary 630 FTIR (Agilent Technologies). The sample was placed on the diamond ATR of the instrument and the peaks were observed using the Microlab PC software.

Disc diffusion assay

As per the previously published protocol of Dey *et al*. 2015, the nutrient broth was prepared and autoclaved at a temperature of 121°C and pressure of 15 lbf/in2, for 20 min. Mother inoculum for both bacterial cultures (*S. aureus* ATCC no. 25923 and *E. coli* DH5α ATCC no. 67877) was taken in 1:100 ratios and the sterile broth was inoculated. The flasks were then incubated overnight in the orbital shaker at 37°C. After 24 h of incubation, the turbidity confirmed the growth of the culture in the media. The absorbance at 600 nM was measured in a UV spectrophotometer and CFU/mL was calculated as:

OD (Optical Density) = 0.8×10^9 CFU/mL. …

The susceptibility of AuNPs against bacteria was assessed by Kirby Bauer method. Briefly, LB agar plates were prepared and the soft agar containing the bacterial suspension was poured on it. Sterile discs of Whatmann's filter paper were then kept on each section, laden with 20 µL of AuNPs, Gentamycin (5 mg/mL) was used here as a positive control and distilled water as a negative control. The plates were then sealed with parafilm and were incubated at 37°C overnight. The zone of inhibition (ZOI) was observed post 24 h and measured subsequently.

Growth kinetics study

Sterile broth inoculated with bacterial culture (*S. aureus* ATCC no. 25923 and *E. coli* DH5α ATCC

no. 67877) approximately 2×10^4 CFU/mL was taken in 96 well plate. 20 uL of the test samples (AuNPs) were added to the respective wells, while the control well contained plain bacterial culture. The effect of the test sample on the bacterial growth kinetics curve was recorded. Absorbance values were measured at 600 nM as a function of time, for both the experimental and the control groups to obtain the growth curves.

Results and Discussion

Various plant parts have been used for the green synthesis of metal nanoparticles Synthesis of AuNPs in a colloidal form is most commonly done by reduction of Auric chloride. The possible mechanism involves the formation of intermediary complexes with the phenolic -OH groups present on the hydrolysable tannins, under-going an oxidation reaction to quinine followed by reduction of AuNPs from Au^{+16}. Figure 1 indicates the UV absorption spectra of AuNPs. The formation of AuNPs was characterized by a change from pale yellow $AuCl_4$to a ruby red solution. The appearance of the ruby red colour was a result of the excitation of surface plasmon resonance (SPR), majorly of AuNPs having the λ_{max} in the range of 500-600 nM. On examining AuNP, it was observed that the intensity of the peak was directly proportional to the reaction time, which may be due to the formation of AuNPs during the reaction. It has already been proved that the intensity of the Surface Plasmon peak was directly related to the density of the NPs in solution[17]. The observed SPR was in the range of 500-600 nM and the broadening of the peak indicated the polydispersity of AuNPs[18-20]. Formation of stable AuNPs within an hour proves that this method was an efficient bio-reducing method for synthesizing Au nanostructures. Figure 2 represents temperature dependent variation in the size of the nanoparticles as assessed by dynamic light scattering (DLS) and transmission electron microscopy (TEM) techniques (Fig. 3). TEM measures a number based size distribution of the physical size only. However, DLS is extremely sensitive to even small quantity of large particles which maybe a result of nanoparticles aggregating and thus the DLS peaks are altered by larger sizes. Large particle size in DLS data could be due to hydrodynamic circumference and interaction in various forces in ionic states. Earlier reports also support our results indicating that particle size distribution in DLS data showed size range from 70 nM-125 nM, whereas the TEM data showed a narrow range from 20 nM-50 nM.

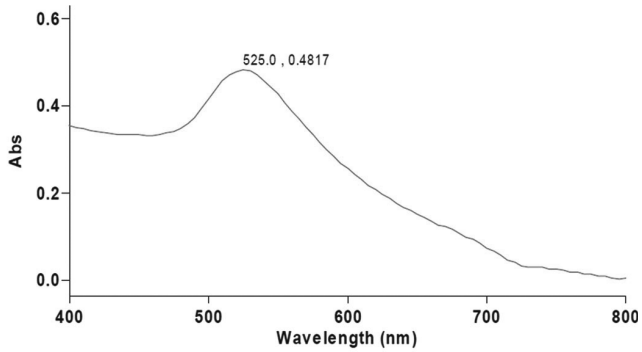

Fig. 1 — Max. Absorption at ~520 nM is characteristic for the formation of gAuNPs

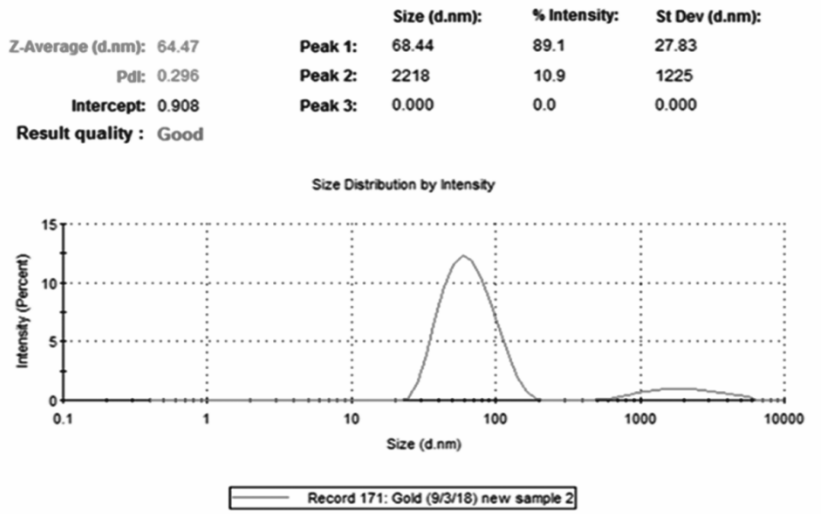

Fig. 2 — Size of AuNPs synthesized from leaves extract of *S. cumini*

Since, the nanoparticles possess a large surface area, the surface modification by a suitable adsorbate can produce different properties, hence FTIR spectroscopy was used for the detection of functional groups in pure compounds, mixtures and for comparison among compounds that correlated with the vibrational motion of atoms or molecules. Figure 4 depicted the FTIR of the AuNP synthesized from *S. cumini* leaf extract that shows the characteristic – CHO peak around 2900 cm^{-1}, C-O stretch of alcohol group at 1100 cm^{-1} and have three peaks depicting amines groups *i.e.* C-N stretch at 1030 cm^{-1}, Ar-N stretch at 1320 cm^{-1} and NH2 in plane bend at 1610 cm^{-1} (Fig. 4). FTIR analysis of *S. cumini* leaf indicated a broad and strong absorption band in a range of 685^{-1} 638 cm^{-1}. These absorptions are allocated to different stretching vibrations. The C-C, O-H stretching vibration appeared at 685 cm^{-1}, 1633 cm^{-1} and 3400 cm^{-1}, respectively. Further, the C=O stretching was observed at 1400 cm^{-1}.

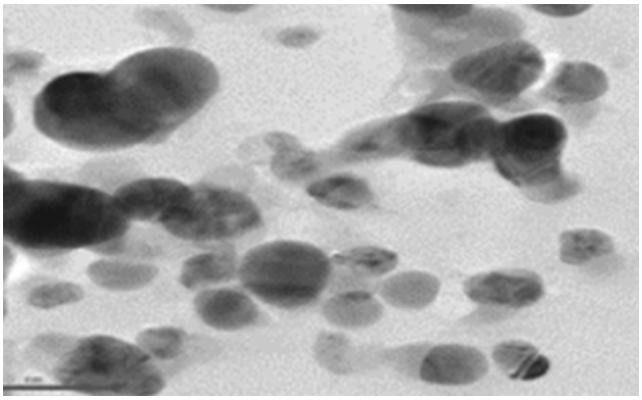

Fig. 3 — TEM images of gAuNPs

Antimicrobial disc diffusion assay of the prepared AuNPs were done (Table 1 and Fig. 5) and antibacterial activity was observed against both Gram positive (*S. aureus*) or Gram negative (*E. coli*) bacteria. Figure 6A and B indicates the growth inhibition curves by AuNP at two different concentrations *i.e* 10 µg/mL and 100 µg/mL on both *E. coli* and *S. aureus* bacteria Time dependent growth inhibitory activity was observed by AuNPs[21].

Literature survey suggests that AuNPs were capable of adhering to the bacterial cell wall and

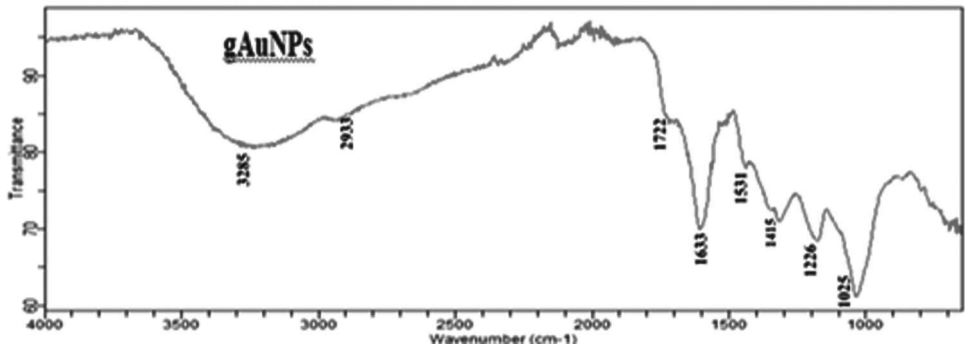

Fig. 4 — FTIR of gAuNPs Peaks at 2933, 1633, 1531 and 1415 cm^{-1} were attributed to the stretching vibrational frequencies of various functional groups such as H of methyl and methoxy groups, C=O of acid derivatives, C=C of aromatic rings and amide groups which come from the biomolecules of *Syzygium cumini*

Fig. 5 — Antibacterial activity of test samples *i.e.* Leaf extract, gAuNPs in gram-positive (*S. aureus*) and gram- negative (*E. coli*) bacteria and its comparison with positive control (Gentamycin 5 mg/mL) & negative control

Table 1 — Antimicrobial disc diffusion assay

Sample	Zone of Inhibition - ZOI (mM)	
	E. coli	*S. aureus*
Positive Control (Gentamycin: 5 mg/mL)	10±0.1	8±0.5
Negative Control	0±0	0±0
Leaf extract	0±0	0±0
gAuNPs	4±0.4	2±0.2
gAuNPs	2±0.2	1.5±0.2

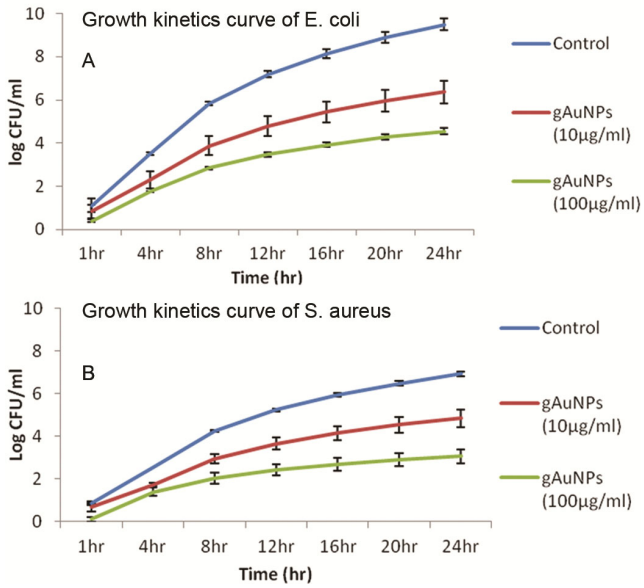

Fig. 6 —Growth kinetics curves of (A) *E. coli*; and (B) *S. aureus* when treated with gAuNP (10 µg/mL) and gAuNP at 100 µg/mL. Values are represented as mean ± standard deviation of three sets of identical experiments

penetrating it, causing conformational changes in the cell membrane ultimately leading to cell death[22]. Published evidences indicated strong interaction between AuNPs and the peptidoglycan (PGN). AuNPs interact with bacterial cell walls individually or *via* the released Au+ ions that generate "pits"in the cell walls owing to their nano size. This leads to the accumulation of AuNPs on the cell membrane as they begin to adhere strongly to the layers, thereby releasing more and more Au^{+}ions. This phenomenon strongly influences the destruction of Gram-positive bacteria as they have a thicker PGN layer, but Gramnegative bacteria are resistant to this phenomenon. According to Reidy *et al*. 2013, there are a series of mechanisms by which the AuNPs manifest their antibacterial property. As nanoparticles have an ultrasmall size and a large surface area, they are capable of makinga strong contact with the bacterial surface. It has been reported earlier that Au-P III inhibited the division in both *S. aureus* and *E. coli*. Secondly, the AuNPs penetrate the bacterial cell wallthat leads to DNA damage. Thirdly, the dissolution of AuNPs releases Au^{+} ions that can act together with sulphur-containing proteins of bacteria to alter the structure and function. This phenomenon is an important mechanism of the antimicrobial activity of AuNP. The interaction of dissolved Au^{+} ions to extracellular as well as intracellular proteins highlights the binding of Au^{+} ions with the thiol group present in the vital enzymes that result in their inactivation or altered activity. Fourthly, Au^{+} ions may further interact with the phosphorous containing compounds like DNA which undoubtedly interferes with its replication process and inhibits the proliferation resulting in decreased growth over a period of time.

Conclusion

We report cost effective, eco-friendly, safe, simple, non-toxic, and single step synthesis protocol for AuNPs from leaf extracts of *Syzygium cumini*. The AuNPs made by leaf extract at 25°C was found to be more active in terms of antimicrobial activity. The efficacy of AuNPs was evident in Gram positive bacteria at nanogram concentrations as compared to Gram negative bacteria, These preliminary results warrant further experiments to elucidate the molecular mechanism both *in vitro* and in *in vivo* models. The proposed cost-effective and eco-friendly approach for mass production of AuNPs has immense potential applications.

Conflict of interest

All authors declare no conflict of interest.

References

1 Yu R, Wu J, Liu M, Zhu G, Chen L, Chang Y & Lu H, Toxicity of binary mixtures of metal oxide nanoparticles to Nitrosomonas europaea.*Chemosphere*, 153 (2016) 187.

2 Vadlapudi V & Kaladhar DSVGK, Review: Green Synthesis of silver and gold nanoparticles. *Middle East J Sci Res*, 19 (2014) 834.

3 Ahmed BA, Raman T & Anbazhagan V, Platinum nanoparticles inhibit bacteria proliferation and rescue zebrafish from bacterial infection.*RSC Adv,* 6 (2016) 44415.

4 Barua S, Banerjee P. P, Sadhu A, Sengupta A, Chatterjee S, Sarkar S & Karak N, Silver nanoparticles as antibacterial and anticancer materials against human breast, cervical and oral cancer cells. *J Nanosci Nanotechnol*, 17 (2017) 968.

5 Liu YC & Lin LH, New pathway for the synthesis of ultrafine silver nanoparticle from bulk silver substrates in aqueous solutions by sono-electrochemical methods, *Electrochem Commun*, 6 (2004) 1163.

6 Tan Y, Wang Y, Jiang L & Zhu D, Thiosalicylic acid-functionalized silver nanoparticles synthesized in one-phase system. *J Colloid Interface Sci*, 249 (2002) 336.

7 Smetana AB, Klabunde KJ & Sorensen CM, Synthesis of spherical silver nanoparticles by digestive ripening, stabilization with various agents, and their 3-D and 2-D superlattice formation), *J Colloid Interface Sci*, 284 (2005) 521.

8 Mallick K, Witcomb M, Scurrell M. S, Green Nanotechnology for Biofuel Production, *Mater Chem Phys*, 90 (2005) 221.

9 Srikar SK, Giri DD, Pal DB, Mishra PK & Upadhyay SN, Green Synthesis of Silver Nanoparticles: A Review. *Green Sustain Chem*, 6 (2016) 34.

10 Remya VR, Abitha VK, Rajput PS, Rane AV & Dutta A, Silver nanoparticles green synthesis: A mini review. *Chem Int*, 3 (2017) 165.

11 Iravani S, Green synthesis of metal nanoparticles using plants. *Green Chem*, 13 (2011) 2638.

12 Swami SB, Thakor NSJ, Patil MM & Haldankar PM, Jamun (*Syzygium cumini* (L.): A Review of Its Food and Medicinal Uses. *Food Nutr Sci*, 3 (2012) 1100.

13 Dey A, Dasgupta A, Kumar V, Tyagi A & Verma AK, Evaluation of antibacterial efficacy of polyvinylpyrrolidone (PVP) and tri-sodium citrate (TSC) silver nanoparticles. *Int Nano Lett*, 5 (2015) 223.

14 Bindhu, M.R & Umadevi M, Antibacterial activities of green synthesized gold nanoparticles. *Mater Lett*, 120 (2014) 122.

15 Ojo OA, Oyinloye BE, Ojo AB, Ajiboye BO, Olayide II, Idowu O & Adewunmi F, Green-route mediated synthesis of silver nanoparticles (AgNPs) from *Syzygium cumini* (L.) Skeels polyphenolic-rich leaf extracts and investigation of their antimicrobial activity. *IET Nanobiotechnol*, 12 (2018) 305.

16 Narang J, Rani K & Singhal C, Green versus chemical synthesis of gold and silver nanoparticles. *J Bionanosci*, 10 (2016) 341.

17 Mittal D, Narang K, Kapinder LA, Kumar K & Verma AK. Elucidation of biological activity of silver Based Plant Using Nanoparticles Constituents of *syzygium cumini* (L.). *Int J Nanosci Nanotechnol*, 15 (2019) 189.

18 Aljabali A, Akkam Y, Al Zoubi M, Al-Batayneh K & Al-Trad B, Abo Alrob O & Evans D, Synthesis of gold nanoparticles using leaf extract of *Ziziphus zizyphus* and their antimicrobial activity. *Nanomaterials,* 8 (2018) 174.

19 Ayyanar M & Subash-Babu P, *Syzygium cumini* (L.) Skeels: A review of its phytochemical constituents and traditional uses. *Asian Pac J Trop Biomed*, 2 (2012) 240.

20 Aromal SA & Philip D, Green synthesis of gold nanoparticles using *Trigonella foenum-graecum* and its size-dependent catalytic activity. *Spectrochim Acta A Mol Biomol Spectrosc*, 97 (2012) 1.

21 Nguyen KT, Targeted Nanoparticles for cancer therapy: promises and challenges, J *Nanomed Nanotechnol*, 2 (2011) 1.

22 Mohanlall V & Biyela B, Biocatalytic and biological activities of *Kigelia africana* mediated silver monometallic and copper-silver bimetallic nanoparticles. *Indian J Biochem Biophys*, 59 (2022) 94.